Development and Application of an Excitation Ratiometric Optical pH Sensor for Bioprocess Monitoring

Ramachandram Badugu, Yordan Kostov, Govind Rao, and Leah Tolosa
Center for Advanced Sensor Technology, Dept. of Chemical and Biochemical Engineering, University of Maryland Baltimore County, Baltimore, MD 21250

DOI 10.1021/bp.66
Published online December 2, 2008 in Wiley InterScience (www.interscience.wiley.com).

The development of a fluorescent excitation ratiometric pH sensor (AHQ-PEG) using a novel allylhydroxyquinolinium (AHQ) derivative copolymerized with polyethylene glycol dimethacrylate (PEG) is described. The AHQ-PEG sensor film is shown to be suitable for real-time, noninvasive, continuous, online pH monitoring of bioprocesses. Optical ratiometric measurements are generally more reliable, robust, inexpensive, and insensitive to experimental errors such as fluctuations in the source intensity and fluorophore photobleaching. The sensor AHQ-PEG in deionized water was shown to exhibit two excitation maxima at 375 and 425 nm with a single emission peak at 520 nm. Excitation spectra of AHQ-PEG show a decrease in emission at the 360 nm excitation and an increase at the 420 nm excitation with increasing pH. Accordingly, the ratio of emission at 420:360 nm excitation showed a maximum change between pH 5 and 8 with an apparent pK_a of 6.40. The low pK_a value is suitable for monitoring the fermentation of most industrially important microorganisms. Additionally, the AHQ-PEG sensor was shown to have minimal sensitivity to ionic strength and temperature. Because AHQ is covalently attached to PEG, the film shows no probe leaching and is sterilizable by steam and alcohol. It shows rapid (∼2 min) and reversible response to pH over many cycles without any photobleaching. Subsequently, the AHQ-PEG sensor film was tested for its suitability in monitoring the pH of S. cereviseae (yeast) fermentation. The observed pH using AHQ-PEG film is in agreement with a conventional glass pH electrode. However, unlike the glass electrode, the present sensor is easily adaptable to noninvasive monitoring of sterilized, closed bioprocess environments without the awkward wire connections that electrodes require. In addition, the AHQ-PEG sensor is easily miniaturized to fit in microwell plates and microbioreactors for high-throughput cell culture applications.

Keywords: pH sensors, optical sensors, ratiometric sensors, allylhydroxyquinolinium bromide, poly(ethylene glycol), yeast fermentation, online measurements

Introduction

The determination of pH is crucial to defining many important chemical or biological processes. In clinical diagnostics, changes in the pH of blood can be an indication of respiratory or metabolic distress.[1] In critical care such as when a nasogastric tube is employed, the gastric pH is monitored to make sure the employed tube is in the right place and the patient is not in danger of adverse conditions.[2–6] The measurement of pH is also important in maintaining food freshness as yeast and bacteria growing in food can produce soluble acids and amines.[7–10] In environmental monitoring, the pH of rain water is a measure of the level of pollution in the air from industrial and automotive exhausts such as sulfur oxides.[11–13] In industrial fermentation and cell culture, control of pH and other parameters is essential to optimum product formation.[14–17] Control of the extracellular pH in cell culture is important because it affects the intracellular pH, cell metabolism, glucose transport, the adenosinetriphosphate/adenosinediphosphate ratio, as well as other processes that contribute to the well being of the cells and the production of the desired cell product.[18] Thus, there are numerous studies on the optimum pH for different cell lines. In general, the optimum pH range falls between pH 4 and 8 for various prokaryotes and eukaryotes that are of value.

For several years, our group has been working on the development of low-cost, noninvasive, and continuous sensor systems to monitor various analytes (including pH, pO_2, pCO_2, glucose, glutamine, etc.) in cell culture.[19–24] Our first pH sensor based on 8-hydroxypyrene-1,3,6-trisulfonic acid, trisodium salt (HPTS) was constructed using noncovalent binding interactions of the anionic HPTS with supporting polyethylene glycol film. To maximize the noncovalent interactions between the dye and the supporting matrix, and minimize the dye leaching, HPTS was electrostatically adsorbed on to anionic exchange Dewex resin that is entrapped in

Correspondence concerning this article should be addressed to L. Tolosa at Leah@umbc.edu.

polyethylene glycol film. Accordingly, thus obtained senor film has shown a useful range of pH 6–9, with an apparent pK_a of 7.60.[22] However, this sensor does show significant photobleaching as well as probe leaching, making it difficult for real-time applications. Several unsuccessful attempts were made to develop immobilizable HPTS without disturbing its pH response. In this regard, we developed a pH sensor using methacrylate derivative of 6,8-dihydroxypyrene-1,3-disulfonic acid, disodium salt (MA-HPDS). The sensor developed with MA-HPDS show very similar pH response to that observed with HPTS.[23] However, the sensor films constructed using MA-HPDS show significant photobleaching similar to that observed with HPTS-based sensors. In addition to this, we observed distinctly different photobleaching kinetics from the corresponding acid and conjugate base species of HPTS and MA-HPDS, affecting the ratiometric response of the constructed sensors. Here we report a new pH sensor using a covalently immobilizable pH responsive probe that has high stability for long periods of photoilluminations with a slightly more acidic useful pH range (pH 5–8).

Traditionally, pH monitoring is performed using well-established electrochemical sensors. However, using these sensors in certain applications can be problematic if not impossible. Although bioreactors with capacities of 1 L or more are equipped with pH electrodes, it is difficult to do the same for small scale fermentations such as microbioreactors ($\leq$50 mL) or multiwell plates. Thus, monitoring high-throughput bioprocessing is difficult. Additionally, attaching a pH meter to shake flasks presents multiple difficulties including expense, changes in mixing dynamics, and potential release of electrode solution into the media. On the other hand, optical pH sensors offer promising alternatives.[25–34] Most optical pH sensors consist of a pH-sensitive fluorescent dye that can be immobilized, physically or chemically, to a suitable proton-permeable polymer matrix that is then affixed to the inner wall of the glass container. In this way, the sensor patch is continually awash in the cell culture media. For signal detection, an externally mounted monitoring device collects the signal changes from the sensing patch, which are then analyzed. Accordingly, change in broth pH can be followed from the exterior surface, noninvasively and continuously during the entire course of the fermentation process. We have made reasonable progress in developing hand-held, portable, LED-based devices that send and collect excitation and emission light to and from the indwelling sensor film from the surface of the bioreactor.[20–24] For the present pH sensor, we tried a different approach that allows for the use of a tabletop fluorescence spectrometer. In this method, pH measurements were continuously taken by using a closed loop tube that circulates the fermentation broth to and from the bioreactor and the sampling unit (a cuvette in the sample holder of the spectrofluorimeter). This way we are able to more fully characterize the sensor by observing changes in the whole spectrum rather than monitoring at the two excitation wavelengths only. Nonetheless, a simple device is now under construction.

Numerous fluorescence sensors have been developed that measure the pH-dependent change in emission intensity.[30–33] However, most often, these intensity-based measurements suffer from inherent drawbacks due to probe photobleaching, leaching of the probe into the solution, heterogeneity of the probe concentration in the matrix, fluctuations in the intensity of the light source, and change in medium transparency.

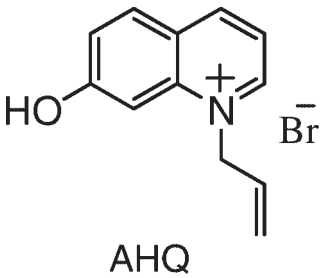

Figure 1. Molecular structure of *N*-allyl-7-hydroxyquinolinium bromide (AHQ).

This is especially problematic during the fermentation process where an increased cell-mass amplifies the scattering or fluorescence from the medium.[34] This gives rise to significant artifacts in fluorescence intensity based pH monitoring. Lifetime-based sensors, whose fluorescence lifetimes are pH-dependent, do not suffer from these same drawbacks but require more complicated and expensive instrumentation.[35]

An alternate approach that circumvents the problems associated with intensity-based measurements is ratiometric detection. Given a fluorescent indicator that exhibits a pH-dependent shift in excitation or emission wavelength, the ratio of the emission intensity at the two wavelengths can be used as a robust measure of the pH that is insensitive to most of the systematic errors associated with intensity-based measurements. Several ratiometric sensor systems have been described, which rapidly and reliably correlate intensity ratio to the pH of the medium.[36–41] Unfortunately, most of these systems including those developed with HPTS show extensive photobleaching.[22,23] Although the observed photobleaching is accounted for by the ratiometric approach, the useful life-span of these sensors is limited by a progressively decreasing signal. More importantly, these dyes were developed primarily for assay-based measurements and are often tedious or unworkable to immobilize for real-time sensing applications. Sometimes the probe has to be modified for covalent immobilization, but once immobilized, it becomes insensitive to pH. In this regard, we recently designed a new probe, allylhydroxyquinolinium bromide (AHQ) that shows excitation ratiometric pH response with an apparent pK_a of $\sim$6.40 at room temperature. This is in agreement with that of 1-methylhydroxyquinolinium iodide reported earlier.[41] The molecular structure of the AHQ is shown in Figure 1. The probe AHQ is strategically designed to have a pendant allyl group for immobilization on polyethylene glycol dimethacrylate (PEG) and a highly fluorescent pH responsive hydroxyquinolinium moiety. Interestingly, AHQ pH response is insensitive to the matrix polarity and composition, ionic strength, and temperature of the medium. Once immobilized in PEG, the resulting film is resistant to high pressure steam and alcohol sterilization, which makes it particularly useful in bioprocessing. These unique pH response features and utility of AHQ-PEG film as sensor for online pH monitor of yeast fermentation is described in this article.

Experimental Methods

The probe AHQ was prepared using a previously published procedure that describes the synthesis of quinolinium-based boronic acid derivatives developed for glucose sensing.[42,43] Polyethylene glycol dimethacrylate with an average

molecular weight of 1,000 was obtained from Polyscience (Warrington, PA). Reagent grade 7-hydroxyquinoline, allylbromide, dimethylformamide, ammonium persulfate (APS), *N*,*N*,*N*′,*N*′-tetramethylethylenediamine (TEMED), ethylene glycol dimethacrylate, and analytical grade sodium acetate, acetic acid, mono- and dipotassium hydrogen phosphates, sodium carbonate, sodium bicarbonate, glucose, ammonium chloride, magnesium sulfate nonahydrate, and calcium chloride dihydrate were purchased from Sigma-Aldrich. Yeast extract used in the preparation of nutrient broth for yeast formation was obtained from Fischer Scientific. White microfiltration (Nongauze milk-filter; KenAG, Ashland, OH) membrane was used as supporting and blocking aid. Deionized water, purified using a Millipore Milli-Q gradient system with a resistivity of 18.2 MΩ cm, was used in this study.

The AHQ-PEG sensor was fabricated using a previously published procedure with slight modifications suitable for this study.[22,23] Briefly, the prepolymer mixture consisting of polyethylene glycol dimethacrylate, ethylene glycol dimethacrylate (a cross linker), AHQ, and 10% aqueous APS solution in aqueous-ethanol was vortexed vigorously for about 5 min. Subsequently, the mixture was purged with nitrogen gas for about 10 min, followed by the addition of TEMED. Then the mixture was vortexed gently for about a minute before being cast on a cellulosic membrane backing (3 × 4 in.) The backing membrane utilized here is commonly used to filter dairy milk and it will be referred to from here on as milk-filter. The milk-filter membrane is held in place between two glass plates with Teflon spacers. Polymerizing between the two glass plates helps keep an oxygen-free environment for the reaction while ensuring a uniform film thickness as determined by the spacers. Free-radical polymerization of the acrylate end groups were initiated by the added APS and TEMED in the prepolymer mixture. After allowing polymerization to proceed for about 1 h at room temperature, the AHQ-PEG film now firmly affixed to the milk-filter membrane was peeled off from the glass plates. The sensor film was allowed to hydrate in deionized water for overnight. The sensor film was washed thoroughly with solvents in this order: water, methanol, acetic acid, and water, followed by autoclaving. Finally the autoclaved film was washed with copious amounts of sterile deionized water. The sensors constructed in this manner were ~250 μm thick.

For comparison, the control PEG-films without AHQ were also prepared. The sensor films were stored in deionized water until ready for use. To facilitate insertion of the sensor into 3-mL fluorescence plastic (polystyrene) cuvettes for reproducible analysis, the AHQ-PEG film was cut into 1.1 × 2.5 cm^2 pieces. These membrane-backed stiff films are positioned diagonally into the cuvette in the appropriate medium for all fluorescence measurements in buffer. The emission light is collected from the back of the film while illuminating from the front. The excitation spectra were collected at the fixed emission wavelength of 520 nm and slit-widths of 5 nm.

Fluorescence measurements were performed using a Varian Cary Eclipse fluorescence spectrophotometer. A regular cuvette holder equipped with a temperature controllable thermocouple connected to a Peltier cooling system is used for all fluorescence measurements, including the temperature-dependent studies. All experiments other than those at varying temperatures were carried out at 25°C ± 2°C. Uncorrected excitation and emission spectra of both solutions and sensor assemblies were recorded in polystyrene disposable cuvettes. To measure the response time of the sensor, 50 mL buffer solutions were continuously pumped from reservoirs into a sealed cuvette containing a sensor assembly.

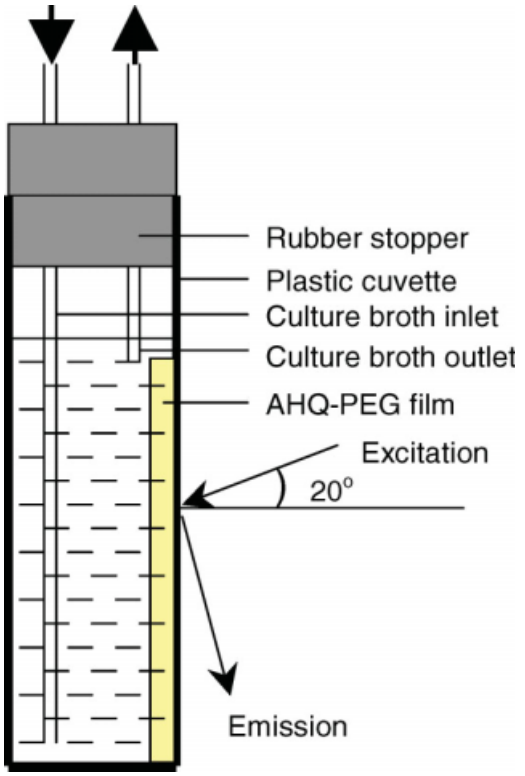

Figure 2. Schematic representation of cuvette with front-face illumination and emission collection to monitor the online pH of yeast fermentation.

For pH calibration of the sensor, buffered solutions (0.1 or 0.005 M overall ionic strength) of sodium acetate-acetic acid (for pH range of 1–4), potassium mono- and di-basic phosphates (for pH range of 5–8), and sodium carbonate-bicarbonates (for pH range of 9–13) were prepared using standard procedures. The pH adjustment to reach pH 1 and pH 12 and 13 were made with 1 N aqueous solutions of HNO_3 and NaOH, respectively. The other buffers were adjusted to whole numbers with corresponding conjugate base or acid. For each set of conditions, the collected data were fit to Eq. 1.

$$R = \frac{[H^+]R_{min} + k_{a,app}R_{max}}{k_{a,app} + [H^+]} \quad (1)$$

using a least-squares linear regression to determine the parameters R_{min}, R_{max}, and $k_{a,app}$.[44]

In the fermentation experiments, the fluorescence and/or scatter contribution from the produced cell mass in the fermentation broth is minimized by front-face illumination.[34] The emission was collected from the surface of the sensor film that is firmly attached onto the inner surface of the cuvette. The schematic representation of the film orientation used for front-face illumination is shown in Figure 2. The fluorescence spectral measurements for online pH monitoring during the fermentation process were performed using a sample/cuvette holder particularly designed for front-face measurements. The excitation light is fixed at an angle of

incidence of 20° to the surface normal. Additionally, to prevent optical interference from the media beyond the edges of the sensor, the outside of the cuvette was masked with a black tape (not shown in the Figure 2, for clarity) except for a small square that exposed the sensor. The culture broth was continuously circulated to and from the shake flask to the cuvette using a peristaltic pump (Fisher Scientific) operating at a speed of 5 mL/min. The yeast nutrient broth (YPD) as prepared contained glucose (15.0 g/L), yeast extract (7.0 g/L), NH_4Cl (2.5 g/L), KH_2PO_4 (1.0 g/L), $MgSO_4 \cdot 7H_2O$ (0.3 g/L), and $CaCl_2 \cdot 2H_2O$ (0.1 g/L) with pH adjusted to 7.0 using 10% NaOH.[45] The pH of each solution was recorded using a model AR 25 Benchtop/Portable Accumet Research Dual channel pH/ion meter (Fischer Scientific). The fermentation was carried out at 37°C in a 500-mL shake flask containing 250 mL of YPD broth that was inoculated with about 100 mg of yeast powder. The shake flask was placed on a rotating shaker (Labline Orbit Environ Shaker; Lab-Line Instruments, Melrose Park, IL) set at 200 rpm. Dissolved oxygen and pH were not controlled. Although steam sterilized sensor film was used, the polystyrene disposable cuvette containing a sensor assembly, closed-loop of nylon tubing that is used to circulate the culture media between the sample and the shake flask was first sterilized thoroughly by circulating 50 mL of 70% ethanol–water solution. Subsequently, about 100 mL autoclaved water was circulated to eliminate any leftover ethanol in the tubing and in sampling cuvette. Then the tubing was inserted into the fermentation flask. The fermentation broth was pumped into the cuvette and recirculated to the shake flask by the peristaltic pump operating at a speed of 5 mL/min. The Varian Eclips spectrophotometer recorded the emission intensity at 550 nm with excitation at 360 and 420 nm, at 0.1-min intervals. The ratiometric data collected by the instrument were converted to pH using Eqs. 2 and 3 with the previously determined calibration parameters. At 30-min intervals, samples of the media from the shake flask were removed and analyzed for pH using conventional electrochemical probe and optical density (600 nm) using a Agilent UV–visible diode-array absorption spectrophotometer.

Results and Discussion

The polyethylene glycol hydrogel film, as expected, was shown to be a suitable matrix for pH sensing as it is highly hydrophilic with ~85% water content and high proton diffusion coefficients.[46] Polymerization between two glass plates to control the film thickness simplified the molding steps and increased the reproducibility of the measurements. Additionally, the use of the milk-filter membrane as a supporting film increased the strength of the sensing film making it resistant to harsh conditions such as repeated washing with various solvents and buffers and steam sterilization by autoclaving. This white membrane also blocks the interfering signal from the fermentation medium.[34] However, the white milk-filter membranes can potentially contribute to the net fluorescence signal from the sensor assembly, especially in experiments using short excitation wavelengths. In the present case, we see insignificant contribution from the blocking film as well as from the blank PEG film that has no attached dye as shown by the relative emission intensities of AHQ-PEG film and the control PEG film in deionized water (Figure 3). Interestingly, the white, reflective surface of the blocking

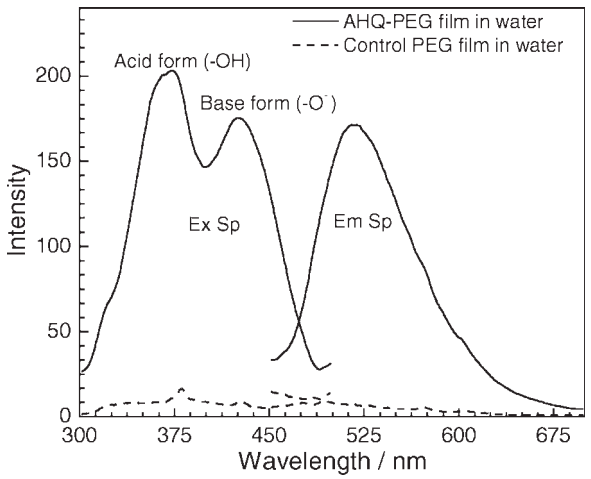

Figure 3. Fluorescence excitation and emission spectra of AHQ-PEG (solid line) and control PEG film (dashed line) films in deionized water with unknown pH.

λ_{em} wavelength for the excitation spectra was 520 nm and λ_{ex} for the emission spectra was 420 nm.

film (while using the film defined in Figure 2) serves to enhance the signal output from the sensor by reflection of both incident and emitted light back through the AHQ layer, rather than allowing transmission beyond the patch. This effectively doubles the path length of the beam, resulting in emission intensities that are up to four times higher than those from similar sensors with no membrane backing.[26]

Figure 3 shows the normalized fluorescence excitation and emission spectra of AHQ-PEG film in water. The sensor film AHQ-PEG in deionized water exhibits two bands (with λ_{max} at ~375 and ~425 nm) in its excitation spectrum. The 375-nm band corresponds to the acid form in which the hydroxyl group of AHQ is protonated as —OH. The 425-nm band is from the corresponding conjugate base that has a deprotonated hydroxyl (or oxy) group, as $—O^-$ or =O.[41] Consistent with other aromatic hydroxy compounds (such as HPTS[47–50] and naphthol[51]), AHQ exhibits increased acidity in the excited state. In other words, AHQ behaves like a "super acid" in the excited state. Correspondingly, the AHQ-PEG film shows a single broad emission band with λ_{max} of 520 nm attributable to the conjugate base of AHQ in water. An analogous spectral behavior was reported previously with a structurally similar compound 1-methyl-7-hydroxyquinolinium iodide in water.[41] Furthermore, the observed two band structure in AHQ-PEG excitation spectra indicates that the two characteristic pH-sensitive excitation wavelengths of AHQ are preserved in the immobilized form. We observed similar response from free AHQ in aqueous buffered solutions (Badugu et al., Manuscript under preparation). Hence, the constructed film is suitable for real-time pH sensing applications.

Figure 4 (top) depicts the pH-dependent fluorescence excitation spectra of the AHQ-PEG sensor film measured at a fixed emission wavelength of 520 nm. The sensor exhibits an increase in the emission intensity with pH with excitations over the isosbestic point (390 nm). On the other hand, the intensity decreases with excitations below 390 nm. We observed over ~20-fold increase in the intensity ratios between pH 5.0 and 8.0 for the blue excitations. This is significantly higher when compared with the response from the HPTS-based sensor. The observed corresponding change in

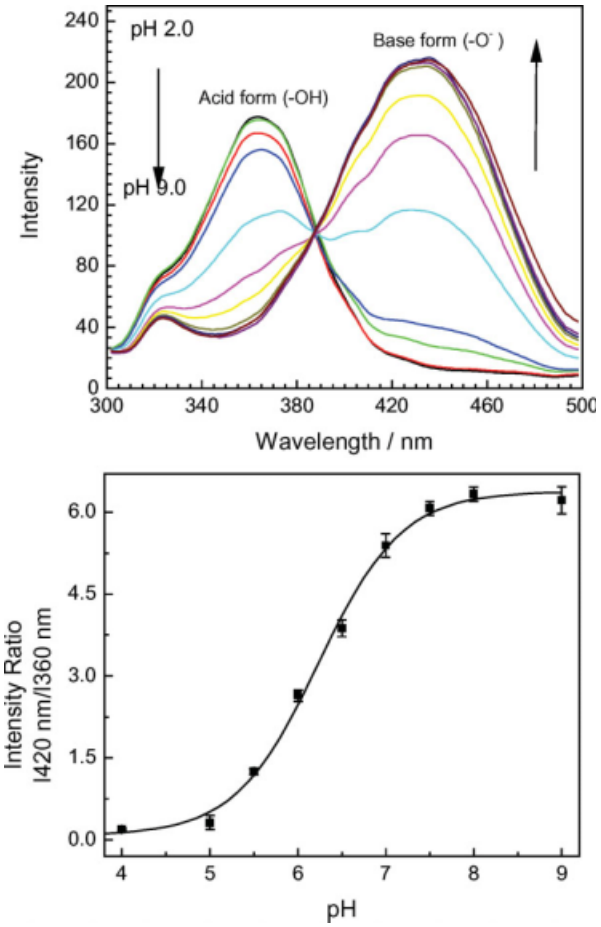

Figure 4. Fluorescence excitation spectra of AHQ-PEG film in different buffer solutions (top) and the sensor intensity ratio with respect to pH of the medium (bottom) (λ_{em} = 520 nm).

intensity ratios for HPTS was about 10-fold.[22] The ratio of the intensities at 420 and 360 nm excitations plotted against pH is shown in Figure 4 (bottom). Multiple separate experiments yielded very similar pH responses, despite slight differences in sensor orientation, thickness, or local probe concentration, demonstrating the reproducibility of sensor construction and the robustness of the ratiometric technique. Very importantly for bioprocess applications, almost the same response was observed with the film before and after autoclaving. In addition, the precision of these measurements indicates that the fluorescence or scatter component from the blocking membrane is consistent and does not interfere with the operation of the sensor.

Subsequently, the ratio of intensities (R) for the two excitation wavelengths (420 and 360 nm) of AHQ-PEG can be related to the proton concentration of the medium by

$$[H^+] = k_a \frac{(R_{max} - R)}{(R - R_{min})} \frac{(\varepsilon_{O^-}\Phi_{O^-})\lambda_2}{(\varepsilon_{OH}\Phi_{OH})\lambda_2} \quad (2)$$

where R_{min} and R_{max} are the ratios for the acid (—OH) and conjugate base (—O^-), respectively, ε and Φ are the extinction coefficient and quantum yield of each species evaluated at λ_2, and k_a is the equilibrium dissociation constant.[44] Experimentally, the apparent dissociation constant $k_{a,app}$, of the immobilized dye, is given by the product

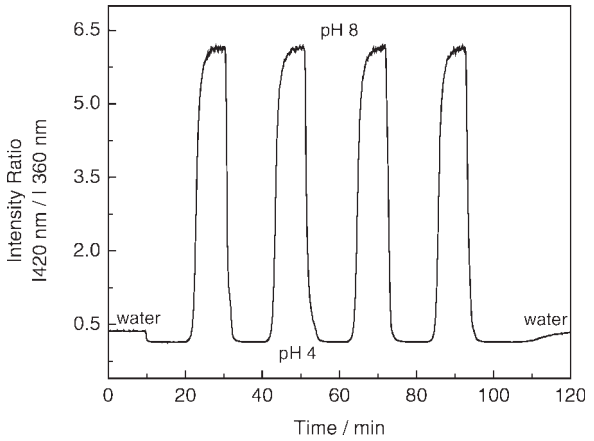

Figure 5. Fluorescence intensity ratio of AHQ-PEG film with time.

The initial and final medium was water and the pH of the medium was changed between pH 4 and 8, alternatively, by pumping 50 mL of buffer solution using a peristaltic pump. The pump speed was 5 mL/min.

$$k_{a,app} = k_a \frac{(\varepsilon_{O^-}\Phi_{O^-})\lambda_2}{(\varepsilon_{OH}\Phi_{OH})\lambda_2} \quad (3)$$

and rearranging Eqs. 2 and 3 gives Eq. 1. Subsequently, the apparent pK_a of 6.40 for AHQ-PEG was deduced by fitting the data in Figure 4 (bottom) to Eq. 1. The range of linearity of the AHQ-PEG sensor extends from ~5.0 to 8.0 and is therefore favorable in terms of bioprocess monitoring, as it corresponds to a working range that is consistent with that observed during many microbial and mammalian fermentations.

The reversibility and dynamic behavior of the sensor was investigated by pumping different buffers (pH 4 and 8) alternatively into the cuvette, using a peristaltic pump with a pumping speed of 5 mL/min. Initially, 50 mL of water was pumped through the cuvette with the AHQ-PEG film. This is followed by alternate solutions of pH 4 and 8. Finally, 50 mL water was pumped to regenerate the sensor film. The pH-induced change in intensity ratio of the AHQ-PEG film with time is shown in Figure 5. The response time for a 95% change was ~2 min. While this is adequate for the purpose of bioprocess monitoring, the faster response times that are desirable for control schemes should be easily attained with a reduction in sensor thickness and increasing the pump speed. As can be seen from the figure, the change in intensity ratio was completely reversible and could be cycled back and forth with no observable drift, *i.e.*, the signal returned to within <1% of the original value with each cycle.

As mentioned earlier, the optical pH sensors (irrespective of their certain limitation such as working pH range) can be easily miniaturized and are not subject to electrical or magnetic interferences whilst attaining better resolutions over electrochemical sensors. However, most optical sensors can be greatly affected by the ionic strength of the medium.[25,52–55] Considering this known fact, we evaluated the effect of buffer ionic strength on the AHQ-PEG sensor. Figure 6 (top) shows intensity ratios of AHQ-PEG sensor obtained in two different (0.005 and 0.100 M) buffers at room temperature. Contrary to our expectations, the intensity ratio of AHQ-PEG showed a smaller dependence on the ionic

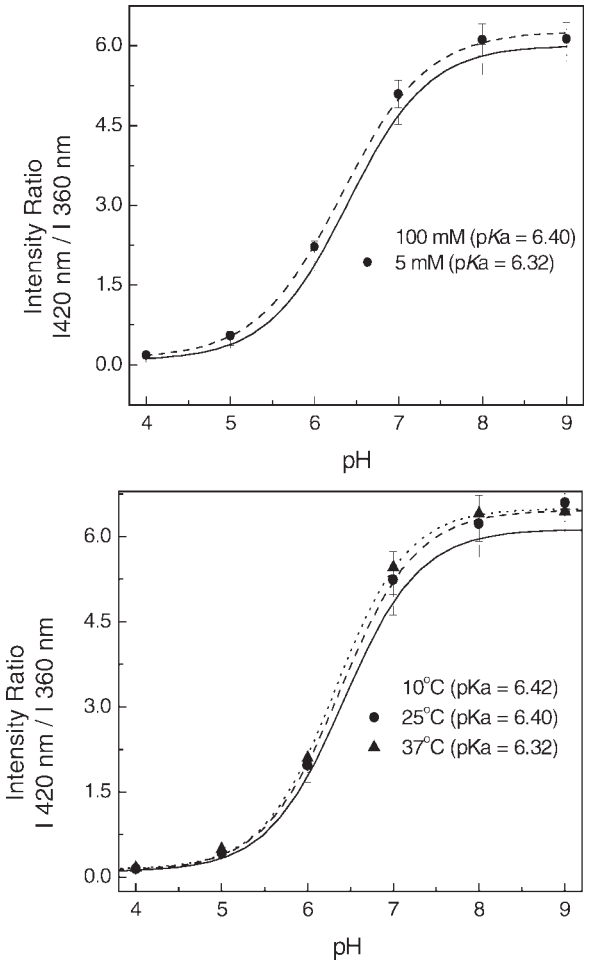

Figure 6. Effect of ionic strength (top) on the pH response of AHQ-PEG film at 25°C (top) and the temperature effect on the film in 0.1 M buffered solutions (bottom).

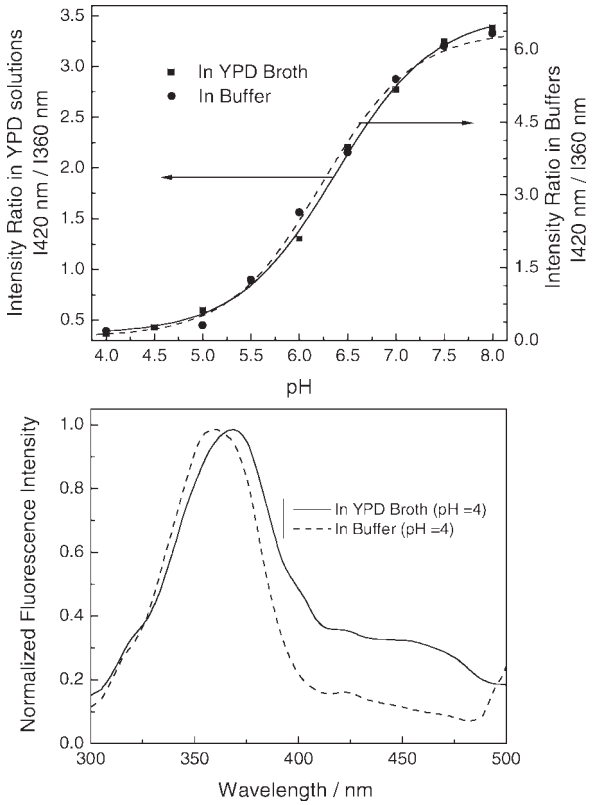

Figure 7. pH response of AHQ-PEG film in clear buffer solutions and in YPD broth (OD_{600nm} = 0.3) at room temperature (top). Bottom panel shows the normalized fluorescence excitation spectra of AHQ-PEG film in clear buffer and YPD broth of pH 4 (λ_{em} = 520 nm).

strength of the buffer than those of HPTS.[22] The apparent pK_a of AHQ-PEG changed from 6.40 to 6.30 when the buffer concentration is reduced from 0.1 to 0.005 M. This observed low cross-responsive nature of the sensor to the ionic strength is yet to be understood. A more detailed investigation is underway (Badugu et al., Manuscript under preparation).

Considering that the temperature can influence the acid dissociation constant of most fluorescent pH sensors, we further tested the effect of temperature on the pH response of AHQ-PEG. As shown in Figure 6 (bottom), AHQ-PEG shows very similar pH responses at three different temperatures: 10, 25, and 37°C. The apparent pK_a of AHQ-PEG film at 10, 25, and 37°C are 6.42, 6.40, and 6.32, respectively. We observed a slight reduction in the intensity ratio at 10°C (see Figure 6, bottom). This discrepancy in intensity ratio might be due to a decrease in acid dissociation efficiency at reduced temperatures. Thus, the reduced sample temperature resulted in increased signal from the acid form affecting the overall intensity ratio. Nevertheless, sensor response is almost identical at both 25 and 37°C, which are the more useful temperatures in bioprocessing. More importantly, as the sensor is targeted for temperature-controlled processes, the pH response can be easily standardized for that specific application.

Although we observed a negligible fluorescence contribution from the supporting milk-filter membrane toward the AHQ-PEG sensor response in clear buffered solutions (Figure 3), we anticipated that the contribution from biological samples, including the produced cells and nutrient broth might be large. Thus, we reestablished the pH responsive curve in the media to help in predicting the pH response data more accurately during fermentation. Correspondingly, the performance of the AHQ-PEG sensor was evaluated in YPD nutrient broth with varied pH (from pH 4 to 8) using the experimental setup shown in Figure 2. Figure 7 compares the intensity ratio of the sensor measured in the YPD broth with the calibration curve in clear buffer. To have better comparison, we obtained a new pH calibration curve for the sensor in clear buffer solution using similar experimental setup. Although the apparent pK_a of the sensor was preserved, the dynamic range [intensity ratio (I_{420}/I_{360})] of the sensor is reduced to half in YPD media when compared with that in clear buffer. This might be largely due to the significant absorption contribution from the YPD broth. The normalized fluorescence excitation spectra of the AHQ-PEG film in clear buffer and YPD broth are shown in Figure 7 (bottom). As can be seen from the figure, the fluorescence excitation spectrum of the sensor AHQ-PEG in YPD shows an additional band at about 450 nm that is contributed by the used broth. Whereas, the corresponding excitation spectra of the sensor film in clear buffer shows no such additional peak. Subsequently, we believe that our attempts to block the background signal (using the opaque milk-filter membrane) is not totally effective. Although milk-filter membrane is more rigid than Whatman filter paper, it is less opaque. Thus, it allows the transmission of about 1% light which is

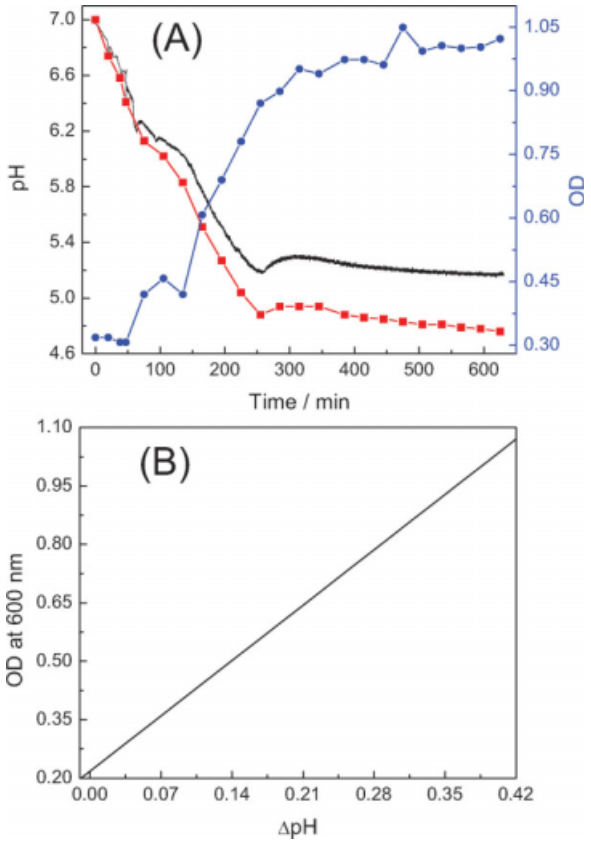

Figure 8. (A) Variation in the pH of the yeast culture during the course of fermentation: measured offline (red) using conventional pH meter and online (black) with AHQ-PEG pH patch. Blue curve shows the increase in OD at 600 nm with time indicating the increase in cell mass with fermentation process. (B) Linear regression obtained between OD vs. ΔpH indicates that the deviation between online and offline pH measurements is indeed due to the increased contribution from the background fluorescence from the cells.

over 10-fold more than that of the Whatman filter paper used in the previous HPTS-based pH sensor.[22] As a consequence, a fraction of both the incident light and the emitted light are lost into the YPD broth. However, the rigidity of the milk-filter membrane provides better mechanical support eliminating the need for the additional plastic (transparency film) support used in the earlier design. Subsequently, eliminating this additional supporting layer allowed for steam-sterilization of the AHQ-PEG film. One way of counteracting the inefficient blocking by the filter membrane is to use higher concentrations of the dye (AHQ) in the sensor patch or adding a second layer of opaque film to the membrane. Also, the background signal can be substantially reduced by using a black light absorbing coating on the rare surface of the sensor film. Despite this drawback with the present design, the ease and simplicity of construction for this sensor film suggest that it is amenable to low-cost, large-scale production. Additionally, because the pK_a remains the same even in media, the applicability to a wide range of cellular bioprocesses is not diminished.

The AHQ-PEG sensor assembly was used to perform continuous online measurement of the pH during *S. cereviseae* fermentation. Figure 8 shows the change in pH of the media recorded online by the sensor and compared with that measured offline by a conventional pH probe with 30-min intervals. Also shown in the figure is the optical density of the media as a measure of biomass production. The fermentation began at pH 7.0 and consistently became more acidic with fermentation time. As the cells enter the exponential growth phase, a dramatic increase in optical density is observed, followed by a corresponding decrease in pH that is consistent with the accumulation of metabolic products such as acetic acid. The ensuing stationary phase is accompanied by a leveling in the pH at ~5.2. On the other hand, the offline pH, measured at 30-min intervals, showed relatively lower pH when compared with that observed with the online measurements, leveling off at about pH 4.7 at the stationary phase. This deviation in the pH measured with two different measurements was ascribed to the increased interference from the produced biomass and relatively less sensitivity of the probe in the acidic pH range (pH $\leq$ 5). However, the observed discrepancy might be largely due to the produced biomass. This is because, as shown in Figure 8B, the ΔpH (i.e. the extent of pH discrepancy between online and offline measurements) is linearly dependent on the amount of produced biomass, quantified using the OD of the fermentation medium at 600 nm. As described earlier while discussing signal contributions from YPD, using much effective background signal masking approaches might provide reduced interference from both the produced biomass and the fermentation broth. By doing so we expect to see an improvement in the dynamic range almost close to that observed in clear solutions (Figure 7) and a reduced discrepancy between the pH observed by offline and online measurements (Figure 8). However, as the interference from the produced biomass has linear tendency, one can easily include a correction factor in generating pH calibration curve used in real-time monitoring device. Nevertheless, it is worthwhile to note that the raw intensities recorded by the sensor, as well as the calculated ratio, were remarkably stable with very little noise and are consistent with the offline measurement, despite the continuous flow of the fermentation broth over 10 h.

Conclusions

The excitation ratiometric pH sensor using a newly developed pH responsive dye AHQ and poly(ethylene glycol) copolymer is described. The sensor AHQ-PEG shows timely and reversible pH response and demonstrates linearity and sensitivity in the physiologically and bioprocess-relevant range with over 20-fold change in intensity between pH 5.0 and 8.0. The pH response of about 2 min was observed at a buffer pump speed of 5 mL/min. The sensor AHQ-PEG showed very minimal dependence to the ionic strength and the temperature of the medium. The developed sensor film is robust, suitable for both autoclaving and alcohol sterilization. The milk-filter membranes used as backing for the AHQ-PEG provided sufficient mechanical support and the simple casting method ensured reproducible results. The sensor was successfully used in a shake-flask setup to provide continuous, noninvasive, online measurements of the pH of yeast fermentation. Although the blocking milk-filter membrane in the present sensor is less efficient in eliminating interferences from the fermentation media, thicker membrane backing should remedy this problem significantly. On the other hand, having a blackening the back surface of the sensing film might reduce the interference from the scattering from the produced biomass. The online pH recorded by the sensor, while slightly higher, kept pace with samples measured

offline with a conventional pH electrode. Accordingly, the present sensor is easily adaptable to monitor sterilized, closed bioprocess environments without the awkward wire connections that electrodes require. Hence, it can be used for disposable bioreactor bags. In addition, the AHQ-PEG sensor is easily miniaturized to fit in microwell plates and microbioreactors for high-throughput cell culture applications. We are currently considering to construct a portable, hand-held, LED-based pH-monitoring device using AHQ-PEG as the sensor film.

Acknowledgments

The authors thank the U.S. Army (Award No. W81XWH-04-1-0781), the National Institutes of Health (Award No. DK062990 and No. DK 072465), and the University of Maryland System, Department of Business and Economic Development (Award No. 0000002881) for the financial support and Mrs. Karuna Mupparapu for some experimental help. Support from Sartorius-Stedim Biotechnology is gratefully acknowledged.

Literature Cited

1. Badonnel Y, Crance JP, Bertrand JM, Panek E. Determination of pH, carbon dioxide tension, and oxygen tension by micro methods. *Pharmacien Biologiste (Paris)*. 1969;6:149–154.
2. Durham RM, Weigelt JA. Monitoring gastric pH levels. *Surg Gynecol Obstet*. 1989;169:14–16.
3. Kristensen M. Continuous intragastric pH determination. I. pH of the gastric juice determined *in situ* and following aspiration. *Den Acta Med Scand*. 1965;177:415–425.
4. Davydov LN. Hydrogen electrodes for the determination of pH and potentiometric titration. *Laboratornoe Delo*. 1960;6:54–57.
5. Lin C-Y. A simple glass-electrode system for the determination of pH of blood and other biological fluids with temperature control. *J Sci Inst*. 1944;21:32.
6. Grant SA, Bettencourt K, Krulevitch P, Hamilton J, Glass R. *In vitro* and *in vivo* measurements of fiber optic and electrochemical sensors to monitor brain tissue pH. *Sens Actuat B*. 2001;B72:174–179.
7. John GT, Goelling D, Klimant I, Schneider H, Heinzle E. pH-Sensing 96-well microtitre plates for the characterization of acid production by dairy starter cultures. *J Dairy Res*. 2003;70:327–333.
8. Young OA, Thomson RD, Merhtens VG, Loeffen MPF. Industrial application to cattle of a method for the early determination of meat ultimate pH. *Meat Sci*. 2004;67:107–112.
9. Canete F, Rios A, Luque de Castro MD, Valcarcel M. Determination of analytical parameters in drinking water by flow injection analysis. Part 1: Simultaneous determination of pH, alkalinity, and total ionic concentration. *Analyst*. 1987;112:263–266.
10. Dybko A, Wroblewski W, Maciejewski J, Romaniuk R, Brzozka Z. Fiber optic probe for monitoring of drinking water. *Proc SPIE*. 1997;3105:361–366.
11. Marinenko G, Koch WF. A critical review of measurement practices for the determination of pH and acidity of atmospheric precipitation. *Environ Int*. 1984;10:315–319.
12. Brennan CJ, Peden ME. Theory and practice in the electrometric determination of pH in precipitation. *Atmos Environ*. 1987;21:901ff.
13. Bourilkov J, Belz M, Boyle W, Grattan K. Electrical pH control in aqueous solutions. *Proc SPIE*. 1999;3538:268–277.
14. Harms P, Kostov Y, Rao G. Bioprocess Monitoring. *Curr Opin Biotechnol*. 2002;13:124–127.
15. Jeevarajan AS, Vani S, Taylor TD, Anderson MM. Continuous pH monitoring in a perfused bioreactor system using an optical pH sensor. *Biotechnol Bioeng*. 2002;78:467–472.
16. Weigl BH, Holobar A, Trettnak W, Klimant I, Kraus H, O'Leary P, Wolfbeis OS. Optical triple sensor for measuring pH, oxygen and carbon dioxide. *J Biotechnol*. 1994;32:127–138.
17. Agayn V, Walt DR. Fiber-optic sensor for continuous monitoring of fermentation pH. *Bio/Technol*. 1993;11:726–729.
18. Hyder A, Laue C, Schrezenmeir J. Effect of extracellular pH on insulin secretion and glucose metabolism in neonatal and adult rat pancreatic islets. *Acta Diabetol*. 2001;38:171–178.
19. Rao G, Bambot SB, Kwong SCW, Szmacinski H, Sipior J, Holavanahali R, Carter G. Application of fluorescence sensing to bioreactors. In: Lakowicz JR, editor. *Topics in Fluorescence Spectroscopy*, Vol.4. New York: Springer; 2006:417–448.
20. Ge X, Hanson M, Shen H, Kostov Y, Brorson KA, Frey DD, Moreira AR, Rao G. Comparisons of optical pH and dissolved oxygen sensors with traditional electrochemical probes during mammalian cell culture. *J Biotechnol*. 2006;122:293–306.
21. Vallejos JR, Kostov Y, Ram A, French JA, Marten MR, Rao G. Optical analysis of liquid mixing in a microbioreactor. *Biotechnol Bioeng*. 2005;93:906–911.
22. Kermis HR, Kostov Y, Harms P, Rao G. Dual excitation ratiometric fluorescent ph sensor for noninvasive bioprocess monitoring: development and application. *Biotechnol Prog*. 2002;18:1047–1053.
23. Kermis HR, Kostov Y, Harms P, Rao G. Rapid method for the preparation of a robust optical pH sensor. *Analyst*. 2003;128:1181–1186.
24. Hanson MA, Ge X, Kostov Y, Brorson KA, Moreira AR, Rao G. Comparisons of optical pH and dissolved oxygen sensors with traditional electrochemical probes during mammalian cell culture, *Biotechnol Bioeng*. 2007;97:833–841.
25. Narayanaswamy R, Wolfbeis OS. *Optical Sensors, Industrial, Environmental and Diagnostic Applications*. New York: Springer; 2004.
26. Lakowicz JR. *Topics in Fluorescence Spectroscopy*, Vol.4. New York: Springer; 2006.
27. Peterson JI, Goldstein SR, Fitzgerald RV, Buckhold DK. Fiber optic pH probe for physiological use. *Anal Chem*. 1980;52:864–869.
28. Zhujun H, Seitz WR. A fluorescence sensor for quantifying pH in the range from 6.5 to 8.5. *Anal Chim Acta*. 1984;160:47–55.
29. Saari LA, Seitz WR. pH sensor based on immobilized fluoresceinamine. *Anal Chem*. 1982;54:821–823.
30. Zen J-M, Patonay G. Near-infrared fluorescence probe for pH determination. *Anal Chem*. 1991;63:2934–2938.
31. Chan C-M, Fung C-S, Wong K-Y, Lo W. Evaluation of a luminescent ruthenium complex immobilized inside Nafion as optical pH sensor. *Analyst*. 1998;123:1843–1847.
32. Price JM, Xu W, Demas JN, DeGraff BA. Polymer supported pH sensors based on hydrophobically bound luminescent ruthenium(II) complexes. *Anal Chem*. 1998;70:265–270.
33. Malins C, Glever HG, Keyes TE, Vos JG, Dressick WJ, MacCraith BD. Sol-gel immobilised ruthenium(II) polypyridyl complexes as chemical transducers for optical pH sensing. *Sens Actuators B*. 2000;67:89–95.
34. Chan C-M, Lo W, Wong K-Y. Application of a luminescence-based pH optrode to monitoring of fermentation by *Klebsiella pneumoniae*. *Biosens Bioelectron*. 2000;15:7–11.
35. Lakowicz JR. *Principles of Fluorescence Spectroscopy*, 3rd ed. New York: Springer; 2006.
36. Salerno M, Ajimo JJ, Dudley JA, Binzel K, Urayama P. Characterization of dual-wavelength seminaphthofluorescein and seminaphthorhodafluor dyes for pH sensing under high hydrostatic pressures. *Anal Biochem*. 2007;362:258–267.
37. Kim S, Pudavar HE, Prasad PN. Dye-concentrated organically modified silica nanoparticles as a ratiometric fluorescent pH probe by one- and two-photon excitation. *Chem Commun*. 2006;2071–2073.
38. Niu CG, Gui XQ, Zeng GM, Guan AL, Gao PF, Qin PZ. Fluorescence ratiometric pH sensor prepared from covalently immobilized porphyrin and benzothioxanthene. *Anal Bioanal Chem*. 2005;383:349–357.
39. Xu Z, Rollins A, Alcala R, Marchant RE. A novel fiber-optic pH sensor incorporating carboxy SNAFL-2 and fluorescent

wavelength-ratiometric detection. *J Biomed Mater Res*. 1998;39:9–15.
40. Song, A.; Parus, S.; Kopelman, R., High-performance fiberoptic pH microsensors for practical physiological measurements using a dual-emission sensitive dye. *Anal Chem*. 1997;69:563–567.
41. Kim GT, Topp MR. Ultrafast excited-state deprotonation and electron transfer in hydroxyquinoline derivatives. *J Phys Chem A*. 2004;108:10060–10065.
42. Badugu R, Lakowicz JR, Geddes CD. Fluorescence sensors for monosaccharides based on the 6-methylquinolinium nucleus and boronic acid moiety: application to ophthalmic diagnostics. *Talanta*. 2005;66:569–674.
43. Badugu R, Lakowicz JR, Geddes CD. Boronic acid fluorescent sensors for monosaccharide signaling based on the 6-methoxyquinolinium heterocyclic nucleus: progress toward noninvasive and continuous glucose monitoring. *Bioorg Med Chem Lett*. 2005;15:3974–3977.
44. Tsien RY. Fluorescent indicators of ion concentrations. *Methods Cell Biol*. 1989;30:127–156.
45. Namdev PK, Thompson BG, Ward DB, Gray MR. Effects of glucose fluctuations on synchrony in fed-batch fermentation of *Saccharomyces cerevisiae*. *Biotechnol Prog*. 1992;8:501–507.
46. Hoffman AS. Hydrogels for biomedical applications. *Adv Drug Del Rev*. 2002;54:3–12.
47. Smith KK, Kaufmann KJ, Huppert D, Gutman M. Picosecond proton ejection: an ultrafast pH jump. *Chem Phys Lett*. 1979;64:522.
48. Tran-Thi TH, Prayer C, Millie P, Uznanski P, Hynes JT. Substituent and solvent effects on the nature of the transitions of pyrenol and pyranine. Identification of an intermediate in the excited-state proton-transfer reaction. *J Phys Chem A*. 2002;106:2244.
49. Tran-Thi TH, Gustavsson T, Prayer C, Pommeret S, Hynes JT. Primary ultrafast events preceding the photoinduced proton transfer from pyranine to water. *Chem Phys Lett*. 2000;329:421.
50. Mohammed OF, Dryer J, Magnes B-Z, Pines E, Nibbering ETJ. Solvent-dependent photoacidity state of pyranine monitored by transient mid-infrared spectroscopy. *Chem Phys Chem*. 2005;6:625.
51. Harris CM, Selinger BK. Proton-induced fluorescence quenching of 2-naphthol. *J Phys Chem*. 1980;84:891–898.
52. Lin J. Recent development and applications of optical and fiber-optic pH sensors. *Trends Anal Chem*. 2000;19:541–549.
53. Wolfbeis OS. *Fiber Optic Chemical Sensors and Biosensors*, Vol. 1. Boca Raton, FL: CRC Press; 1991.
54. Janata J. Do optical sensors really measure pH? *Anal Chem*. 1987;59:1356.
55. Weidgans BM, Krause C, Klimant I, Wolfbeis OS. Fluorescent pH sensors with negligible sensitivity to ionic strength. *Analyst*. 2004;129:645–650.

Manuscript received Nov. 22, 2007, and revision received May 13, 2008.

BTPR0704586